 CMC, vol.31, no.3, pp.157-171, 2012

Deformation Processes of Advanced Alloy in Indentation and Turning

M. Demiral[1,2], A. Roy[1] and V. V. Silberschmidt[1]

Abstract: A comparison of a dynamic indentation method with a quasi-static one is used to study evolution of penetration and a generated force in the indentation process. Turning (a machining process) and dynamic indentation techniques are expected to have similar ranges of strain, strain rate and stress values in the process zone of a workpiece in a case of similar kinematics and boundary conditions. Here, we study the underlying mechanics of these two techniques. Based on advanced finite-element models, similarities and differences between the indentation and turning processes are elucidated.This study demonstrates that some critical cutting parameters can be predicted from indentation process; however, noticeable differences in the underlying deformations do exist.

Keywords: Indentation, Turning, Ti-based alloy, Finite element analysis

1 Introduction

Indentation, due to its experimental simplicity, is commonly used for material characterization [Gouldstone, Chollacoop, Dao, Li, Minor and Shen (2007)]. It is used to probe local material properties, and, potentially, short- and long-range residual stresses at different length scales [Suresh and Giannakopoulos(1998)]. A dynamic indentation technique, compared to a quasi-static one, enables us to measure time-resolved depth and loading responses during the process of indentation [Lu, Suresh and Ravichandrana (2003)]. The underlying deformation mechanisms in a tested material exposed to dynamic loads are sufficiently rich to warrant extensive study on the subject. As a result, various experiments of dynamic indentation has been performed to evaluate material performance under dynamic loading conditions. For instance, Davis and Hunter (1960)and Tirupataiah and Sundararajan (1991) studied a high-strain-rate flow behaviour of a wide range of materials with an impact

[1] Wolfson School of Mechanical and Manufacturing Engineering, Loughborough University, UK
[2] Corresponding author: M. Demiral, E-mail address: V.Silberschmidt@lboro.ac.uk, Tel.:+441509/227566

velocity ranging up to 30 cm/s and 180 m/s; Mok and Duffy (1965) and Lu, Suresh and Ravichandrana (2003) demonstrated that the material's strain-rate sensitivity obtained by means of dynamic indentation was in the same range as that evaluated using other high-strain-rate techniques [Kolsky (1949)] and recently Demiral, Roy and Silberschmidt (2010) demonstrated that there can be noticeable differences in the predicted values of deformation and stress-strain characteristics of the workpiece material depending on different flavours of dynamic indentation such as controlled dynamic and fully dynamic, where the indenter displacement is controlled or not controlled, respectively.

In dynamic indentation values of strains, rate of deformation and stress in the process zone of the workpiece are observed to be highly localized. Interestingly, in machining process, e.g. turning operation, several physical processes such as large plastic deformation of workpiece material, material separation, leading to formation of new surfaces, and complex interaction between the workpiece-chip-tool system itself [Zorev and Shaw (1996)] also lead to highly localized mechanical characteristics. Thus, in light of such similarities, we intend to study these two processes with the intention of trying to use dynamic indentation to predict the material behaviour under dynamic micro impacting machining process such as ultrasonically-assisted turning (UAT) [Ahmed, Mitrofanov, Babitsky and Silberschmidt, V. V. (2007); Astashev and Babitsky (1998)], where thousands of impacts are applied every second by a tool to remove a thin layer of material from the workpiece during machining.

On the other hand, kinematics of dynamic indentation and turning processes differs. In turning, a single-point tool is used to remove a layer of material from the surface of the workpiece forming a 'chip' to obtain a product with the desired dimensions. In dynamic indentation, material displacement without separation is the primary deformation mechanism. Hence, comparing and contrasting these two techniques can allow us to elucidate the specific underlying deformation mechanisms of dynamic indentation and turning processes, especially at the process zone.

In this paper, numerical modelling of various dynamic indentation processes in a Ti-based alloy is carried out with one of the numerical experiment representing a turning process in machining of metals. The overall deformation mechanisms for each are studied to highlight the similarities of, and differences between, the various deformation processes with respect to the exerted forces on the indenter/tool, imposed stresses and temperature distribution in the workpiece material.

2 Methodology

To compare the characteristic features of dynamic indentation and turning processes, three modelling schemes are studied. First, a standard dynamic indentation process is considered, in which an indenter is impressed into a surface of the workpiece as seen in Fig. 1 (referred to as Type I). The indenter angle of $\phi = 45^{\circ}$ with a radius of curvature of its tip of 0.1 mm (Fig. 2) is considered in this study. This corresponds to a cutting tool geometry used in machining of metals [Demiral, Roy and Silberschmidt (2010)]. Next, we simulate a conventional orthogonal turning process, which is commonly performed in machining to study chip formation. In our case it is achieved by changing the position of the tool (indenter) with the same geometry towards one end of the workpiece and then rotating it about the z-axis by an angle of 32.5˚ (referred to as Type T) (Fig. 1). In the machining literature, a relative position of the tool with respect to the workpiece can be explained in terms of rake and clearance angles [Zorev and Shaw(1996)]. Here, the tool has a rake angle α=35˚ and a clearance angle γ=10˚ (Fig. 1). To compare and contrast the dynamic indentation process with turning effectively, a near-edge dynamic indentation (referred to as Type N, Fig. 1) is also considered as a transition from turning to dynamic indentation. In this scheme only the spatial position of the indenter is shifted towards the end of the workpiece. This case is of interest as we intend to study the surface effects (proximity to traction-free boundaries) on a typical dynamic indentation process. In the machining literature the term "tool" is used instead of "indenter"; for all the cases studied here we shall use "indenter", alternatively for "tool".

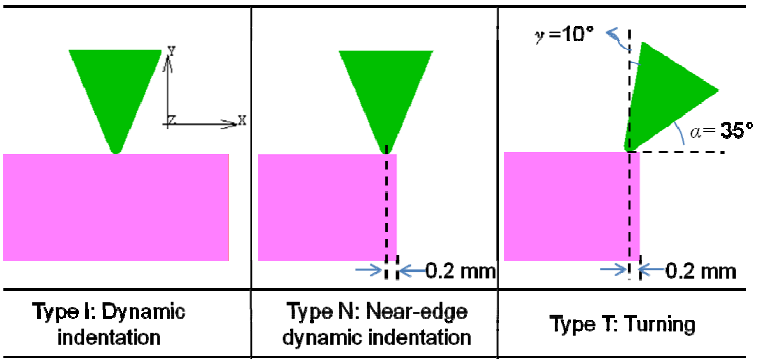

Figure 1: Three modelling schemes

3 Finite-element modelling

Two-dimensional finite-element (FE) approximations of the different modelling paradigms are modelled using the FE software package MSC. Marc [MSC, Marc User's Guide (2011)]. The current FE models are fully transient and thermomechanically coupled in order to correctly account for the interplay between thermal and mechanical processes in deformation zones.

The chosen width of the workpiece is 40 mm for Type I (Fig. 2); for Types N and T it is taken to be 20.2 mm. The height of the workpieces is chosen to be 10 mm for all the cases. In machining, the depth of cut is defined as the distance between the cutting plane (direction of tool path) and the external surface of the layer being removed [Zorev and Shaw(1996)]. In our numerical simulations 0.2 mm depth of cut is considered for the turning operation (Type T). For comparison reasons, in Type N the tool is positioned 0.2 mm from the edge (Fig. 1).

The workpiece material is meshed using a four-noded, isoparametric, quadrilateral plain-strain elements (Element 11). Element sizes of 20 μm, 100 μm and 500 μm are used to discretize various zones of the workpiece as shown in Fig. 2; these elements of different sizes are glued to each other using the "glue" option in MSC. Marc.The selection of elements sizes was based on a mesh-sensitivity analysis aimed at finding a compromise between the conflicting requirements of accuracy and computational cost; it was consistent with the literature data [Garrido Maneiro and Rodriquez (2005); Demiral, Roy and Silberschmidt (2010)]. The finite elements in the primary deformation zone get highly distorted during the deformation processes, which leads to numerical convergence problems and, in some cases, premature termination of the analysis. The problem is sufficiently alleviated with the use of a remeshing criteria, i.e. highly distorted elements are replaced by ones forming a geometrically consistent mesh. Automatic remeshing is defined with a strain-based criterion with a threshold value of 0.4 strain value. In other words, the workpiece is remeshed if the strain change in any element of the current mesh has reached this threshold. The remeshing criterion ensures material separation for types N and T during the deformation process. Kinematic boundary conditions are imposed on the bottom face of the workpiece by constraining displacements in both x- and y-directions (Fig. 2), whereas the top, left, and right faces are free to deform. The details regarding the indenter can be found in reference [Demiral, Roy and Silberschmidt (2010)].

The thermal boundary conditions of the model accounts for convective heat transfer from free surfaces of both the workpiece and indenter to the environment (sinking temperature 20°C) with a heat transfer coefficient of 0.05 W/m^{2}K. Conductive heat transfer due to contact between the indenter and workpiece is represented with a

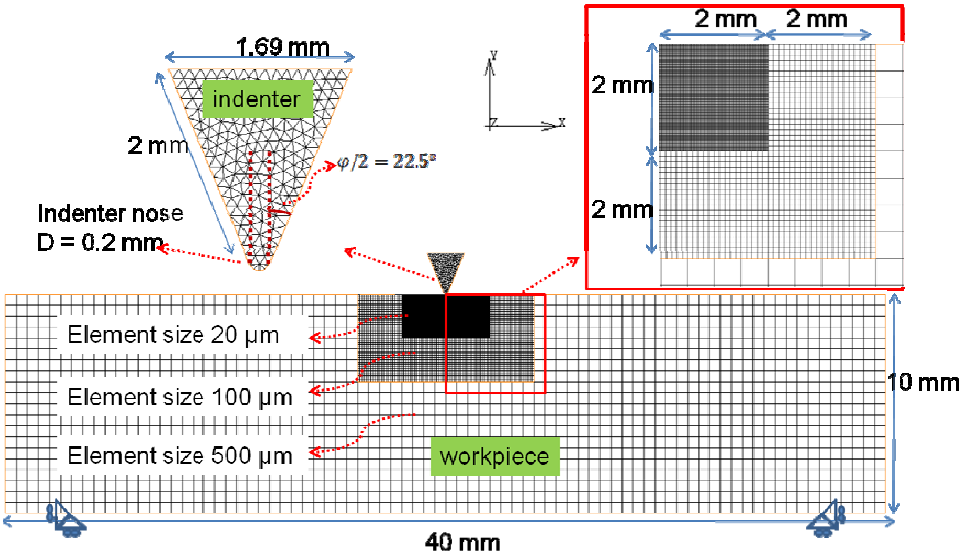

Figure 2: Mesh and boundary conditions used in FE simulations together with enlarged images of indenter and fine-meshed zone

heat transfer coefficient of 50 W/m^{2}K. The workpiece and indenter are assumed to have an initial temperature of 20˚C.

A relative movement of the workpiece and indenter is introduced as a translation of the indenter with a prescribed velocity in the negative direction (Fig. 2). The indenter penetrates 0.51 mm of the workpiece and retracts back from the position of maximum indentation. A back and forth movement of indenter is considered to mimic the tool displacement in ultrasonically-assisted turning. We assume the velocity of indenter to be 20 m/min. This chosen velocity magnitude is representative of the cutting speeds used in a turning process [Zorev and Shaw (1996)]. The dynamic analysis studied here corresponds to controlled dynamic analysis where the deformation process is governed with displacement control of the indenter's displacement. For the detailed analysis regarding the different modelling regimes of indentation process, the reader is referred to reference [Demiral, Roy and Silberschmidt (2010)].

3.1 Material and friction model

A Ti-based superalloy (Ti15V3Cr3Al3Sn) is used as the workpiece material in our simulations. To obtain relevant data on a temperature- and strain-rate-sensitive mechanical behaviour of this alloy, a quasi-static compression test and a split-

Hopkinson test were carried out. The obtained material properties of the alloy are E= 87 GPa, ν = 0.3, ρ = 4900 kg/m^3, where E, ν and ρ are the Young's modulus, Poisson's ratio and density, respectively. The resulting nonlinear material model used in our numerical simulations consists of different stress-strain curves obtained for a combination of different strain rates ($\dot{\varepsilon}$= 0.1 s^{-1}, 1 s^{-1}, 3331 s^{-1}) and different temperature values (20˚C, 600˚C). These curves are modified in such a way that the magnitudes of stresses for high-strain values are limited by the ultimate dynamic tensile stress (UTS) (Figs. 3, 4).

Various frictional models can be implemented possible in finite-element simulations of machining [Ozel (2006); Bahi, Nouari, Moufki, El Mansori and Molinari (2011)]. A shear friction model is adopted in our study owing to its better representation of the friction process [Mitrofanov, Ahmed, Babitsky and Silberschmidt (2005); Ahmed, Mitrofanov, Babitsky and Silberschmidt (2007)]. Two different values of the friction coefficients (μ): μ= 0 (the idealized frictionless condition) and μ = 0.8 (dry condition) are used in the simulations. Further details regarding the material and friction modelling are published elsewhere [Demiral, Roy and Silberschmidt (2010)].

4 Results of simulations and discussion

This part demonstrates the study of the different modelling regimes with regard to the reaction force on the indenter as well as distributions of stresses and temperatures in the deformed workpiece.

One of the main parameters characterising indenter-workpiece interaction is the reaction force since it reflects a global response of the deformed material. Diagrams presenting relationships between the force imposed on the indenter and indentation depth (Fig. 5) are used to compare the deformation process in the workpiece for the studied cases.

It is well known that a dynamic indentation process typically leads to a formation of a 'pile-up', an upward extrusion of displaced material on the surface of the workpiece [Garrido Maneiro and Rodriquez (2005)]. This results in an additional increase of reaction force with an increasing indenter displacement in the dynamic indentation process (Type I). It is observed that the slope of the curve or the rate of increase in force with depth after the initial stage changes at d = 0.04 mm to a lower value (Fig 5). These two different slopes of force-depth diagrams correspond to the transition of the contact face from a circular geometry at the indenter nose to the straight edge of the tool. A similar trend is observed for Types N and T with a change in slope coinciding with the geometric transition of the indenter. The similarity of reaction force values of the processes in Types N and T at the initial

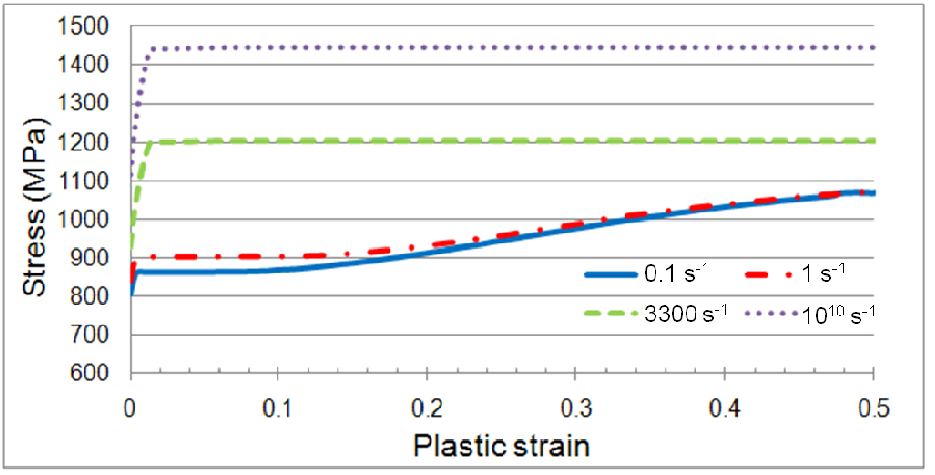

(a)

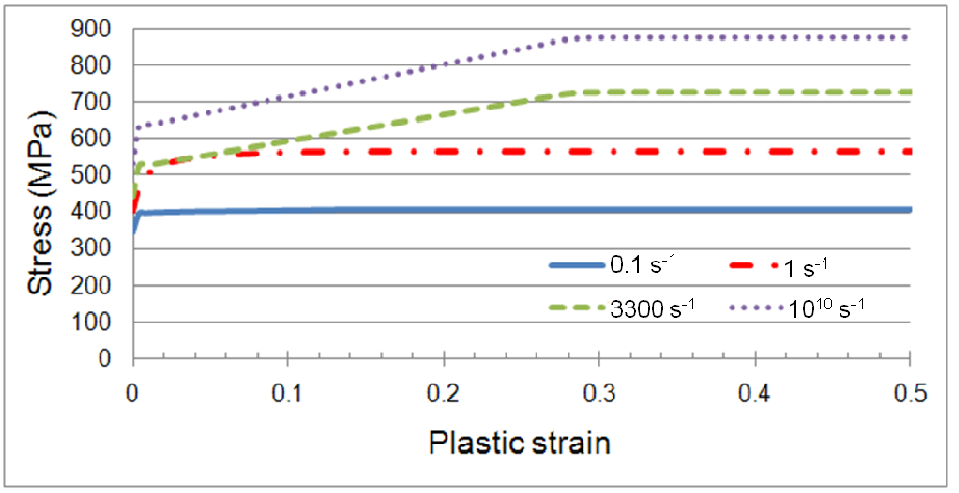

(b)

Figure 3: Modified strain-rate-sensitive material model for 20˚C (a) and 600˚C (b)

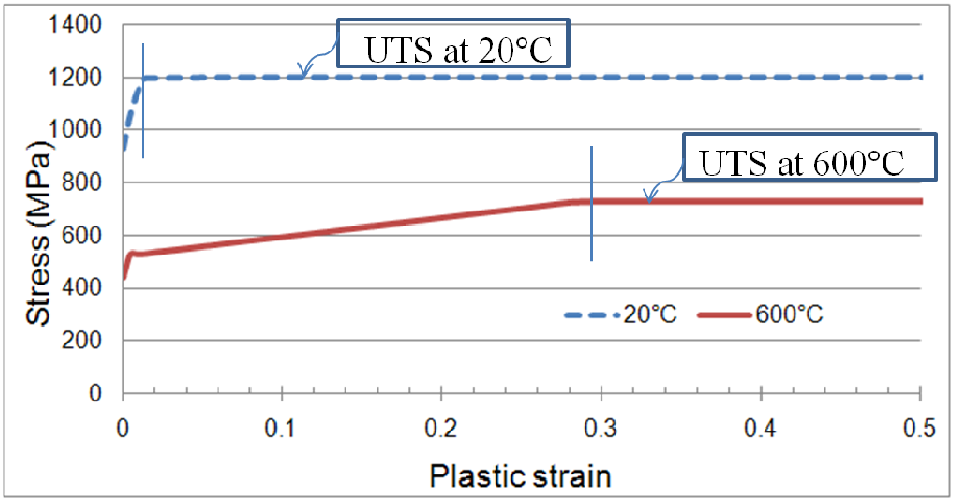

Figure 4: Modified temperature-dependent material model for $\dot{\varepsilon}$= 3331 s^{-1}

phase and the difference when compared with Type I is due to the proximity of the indenter to the traction-free edges of the workpiece. This is observed to be true for both frictional contact conditions (μ= 0.0 and μ= 0.8) (Fig 5).

When considering a near-edge dynamic indentation (Type N), the indenter requires a lower amount of energy for the same level of indenter's displacement than Type I, which reflects on the overall force-depth diagram. This can be explained by the formation of a one-sided pile-up of the workpiece (Fig. 6). On the edge side of deformed workpiece in Type N, the indenter separates its material without any piling-up. It is interesting to note that the one-sided pile up formation contributes substantially to the overall force-depth diagram when compared to a two-sided pile-up deformation process of Type I (Fig 5). In a turning process (Type T) no pile-up formation occurs; instead, the workpiece is deformed and leading to a formation of a "chip" (Fig. 6). It is noted that with an increase of displacement first an increasing reaction force is exerted on the indenter followed by period of its constant level [Zorev and Shaw (1996)]. This is due to the size of the contact length between indenter and the workpiece. The reaction force reaches its constant value when the length of the indenter-workpiece interface has reached its stationary, non-changing size. As the contact length size increases continuously in Types I and N, an increasing reaction force is observed. It should be noted that, in turning, a constant reaction force does not necessarily imply a stationary (equilibrium) chip shape. The chip compression ratio (ratio of chip thickness after turning to undeformed chip thickness) increases continuously for the amount of indenter penetration depth

concerned in this study[1].

Considering the effect of friction for all the cases studied, the relative trend of the force-depth diagrams resembles the frictionless condition (Fig. 5). It is observed that an increase of friction between the indenter and workpiece leads to an increase in reaction force at the maximum indentation depth due to the additional energy required to overcome the frictional forces in dry-contact conditions ($\mu = 0.8$) in contrast to a well-lubricated indenter-workpiece interface ($\mu = 0$) [Demiral, Roy and Silberschmidt (2010)]. The magnitude of reaction force at maximum indentation depth is 451 N (43.9%) higher when a dry frictional contact is assumed compared to frictionless contact condition for Type I (Fig. 7); this value is 143 N (14.7%) and 85 N (23.9%) for Types N and T, respectively. The relative effect of friction on the reaction force of the indenter for various modelling schemes is different. This can be explained by the extent of deformation in the workpiece material during the penetration of the indenter for each case. For Type I, more of the workpiece material as well as the contact length is under the influence of the indenter and thus susceptible to increasing frictional effects.

It is worth mentioning that for different modelling schemes the average strain-rate value near the indenter tip at maximum penetration is observed to be similar with a maximum value of 4000 s^{-1} due to imposed similar kinematics and boundary conditions, consistent with those in [Demiral, Roy and Silberschmidt (2010)]. It is well known that local levels of strain rates in machining processes can potentially reach 10^5 s^{-1} and higher. Our modelling studies are expected to yield similar results for higher deformation studies. A complicating aspect of this modelling regime is the current lack of experimental data at very high strain rates for the material investigated. Calibration of the model to mimic the machining process is left as a topic for a future research.

The effects of different modelling types on the predicted imposed stresses at maximum indentation are also studied. Figure 6 demonstrates the difference in the von-Mises stress for all three types of models. Apparently, deformation process in the immediate vicinity of the indenter in dynamic indentation (Type I) and the material to the left-hand side of the indenter in near-edge dynamic indentation (Type N) are constrained by the bulk of workpiece material and, hence, affected by the indenter's penetration. On the other hand, in the turning regime (Type T) and on the right-hand side of indenter in Type N, the separated part of workpiece is less constrained due to its proximity to the traction-free surface of the workpiece (Fig. 6). The clearance angle of 10° of the indenter in type T allows for the workpiece material to be deformed without a formation of a pile-up in the workpiece. Thus,

[1] We performed additional numerical simulations which demonstrate that a stationary chip shape was obtained at an approximate depth of indenter penetration of 0.75 mm.

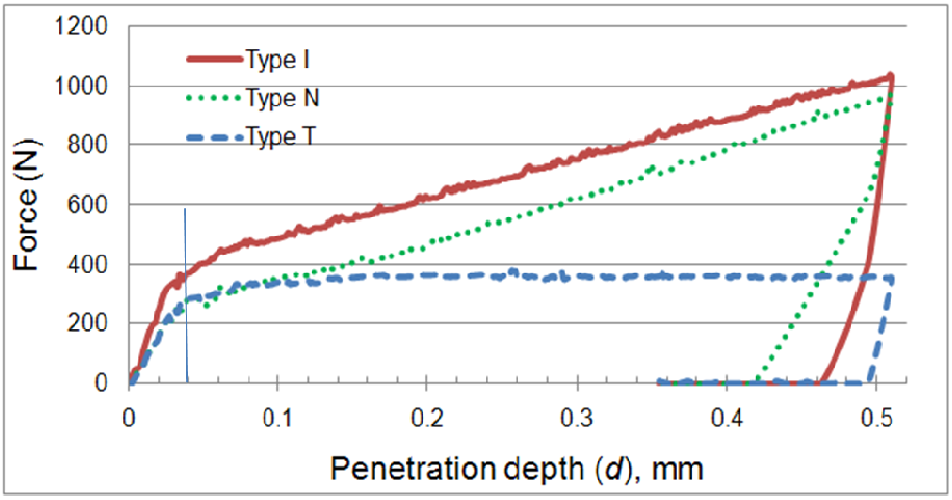

(a)

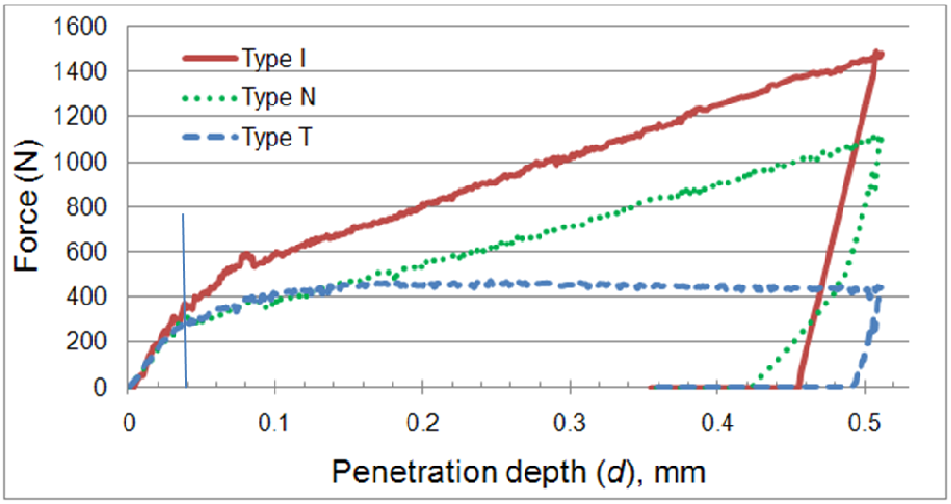

(b)

Figure 5: Evolution of force with penetration depth for various modelled regimes for a perfectly lubricated contact condition ($\mu = 0$) (a) and for dry contact condition ($\mu = 0.8$) (b). The vertical line denotes a transition from a circular geometry of the indenter tip to the straight edge.

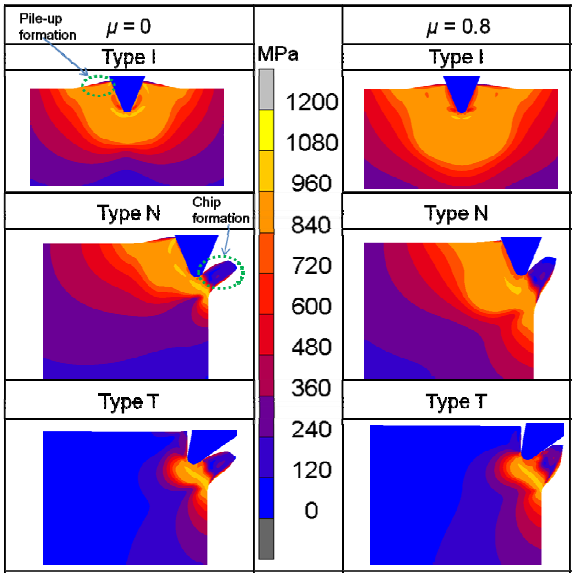

Figure 6: Distribution of von-Mises stress in workpiece at maximum penetration for different modelled schemes. Dimensions of shown parts of workpieces: 4 mm $\times$ 2 mm (Type I) and 2.5 mm $\times$ 2 mm (Types N and T)

the stress values are noticeably larger at the constrained areas of the workpiece as seen for Type I and the left side of Type N when compared to Type T, where the displaced workpiece readily forms a chip.

The stress distributions in the workpiece for different modelling regimes also demonstrate the underlying effects of the kinematics on the deformation process. As the formed chip in turning (T) or in near edge dynamic indentation (N) is free to displace due to its proximity to the traction-free surface of the workpiece, the energy expended by the indenter is considerably less when compared to a classical indentation process (I). Therefore, the separated material from the workpiece experiences smaller stresses when compared to the constrained part.

The frictional conditions affect both the size of the process zone and the overall chip shape in Types N and T. With an increase in friction, the chip adheres to the indenter surface leading to a change in chip morphology (Fig. 6). Such effects are commonly observed in turning of materials.

Obviously, the specific features of realization of irreversible deformation processes for the studied types of indenter-workpiece interaction affect the character of heat generation and, hence, temperature distribution in the deformed material.

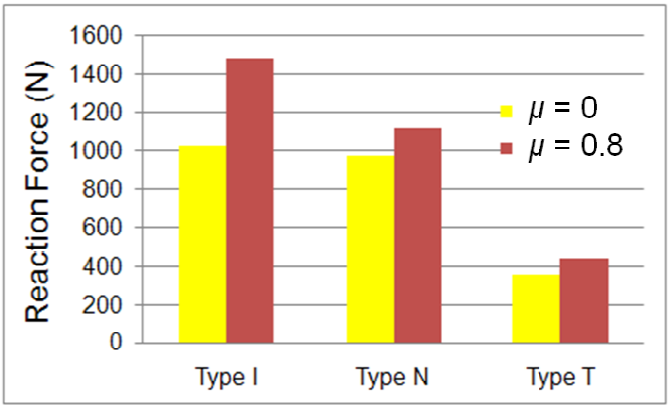

Figure 7: Reaction force magnitude at maximum penetration for different modelled schemes

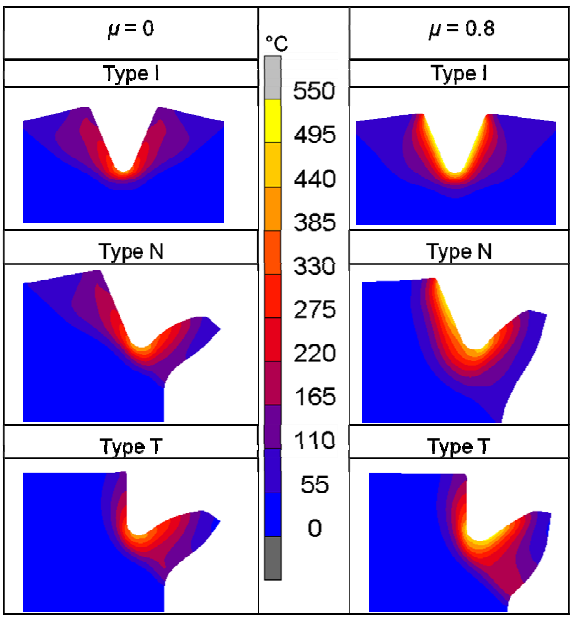

Figure 8: Temperature distribution in workpiece at maximum penetration for different modelled schemes. Dimensions of shown parts of workpieces: 2 mm $\times$ 1 mm (Type I) and 1 mm $\times$ 1 mm (Types N and T)

Due to poor thermal conductivity of the Ti-based alloy (k= 8.08 W m^{-1} K^{-1}), the temperature distribution in the workpiece is highly localized (Fig. 8) when compared to the corresponding stress distribution (Fig. 6). The reduced heat-dissipation rate has consequences for efficient machining of such alloys. The elevated local temperature at the tool-workpiece interface can expedite tool wear. Therefore, advanced high-performance tools with extended endurance and reduced friction should be developed and used to enhance the machinability of such alloys. The temperature values on the left hand-side of the indenter in workpiece (Type T) are smaller compared to those at the same location with respect to the indenter for the other modelling regimes (Types I and N). This is due to the non-zero clearance angle of the indenter in the turning regime, which aids in the increased heat transfer to the ambient environment when compared to other cases. This also influences the overall temperature distribution in the workpiece.

5 Conclusions

Two-dimensional plane-strain FE models of dynamic indentation processes are studied to elucidate the underlying deformation mechanisms for varying indenter orientation and position.

For the dynamic indentation which is closely related to the ultrasonically-assisted turning process, it is observed that the chip-separation process significantly changes the underlying deformation kinematics, resulting in a stress redistribution near the tip of the indenter. As a result, a highly-localized processing zone (known as primary shear zone) is formed, relieving stresses from other parts of the workpiece. Consequently, the deformation zone is comparatively larger in indentation and in near-edge indentation processes. The differences in the underlying deformation processes can be also observed from the reaction force-displacement response of the indenter. A reaction force increasing with displacement is observed to act on the indenter in both the standard indentation and the near edge indentation processes when compared to a turning process, in which the initial stage with a growing reaction force is followed by a stage with a constant one. A retracement of indenter after attaining the maximum indentation depth also demonstrates differences in the force-reduction characteristics.

The similarity of reaction force values of the processes in types N and T at the initial phase is apparent. That can be explained by the proximity of the indenter to the traction free edges of the workpiece. Thus, it is possible to predict the cutting force of a turning process for a ductile material by performing a simple near-edge dynamic indentation test and using the value for a transition to a stage with a lower slope of the force-depth diagram. A standard indentation test (Type I) provides a conservative estimate of the maximum cutting force in the turning process. The

temperature profiles for the various indentation processes studied show a remarkable similarity with each other, in spite of the large difference in the stress distribution profile. This is perhaps due to the low thermal conductivity of the Ti-alloy under study.

In conclusion, the numerical study presented in this paper demonstrates that some critical cutting parameters can be predicted from indentation process; however, noticeable differences in the underlying deformations do exist.

Acknowledgement: The research leading to these results has received funding from the European Union Seventh Framework Programme (FP7/2007-2013) under grant agreement No. PITN-GA-2008-211536, project MaMiNa.

References

Ahmed, N.; Mitrofanov, A.V.; Babitsky, V. I.; Silberschmidt, V. V. (2007): Analysis of forces in ultrasonically assisted turning. *J. Sound Vibrat.* , vol. 308, pp. 845-854.

Astashev, V.K.; Babitsky, V.I. (1998): Ultrasonic cutting as a non-linear (vibro-impact) process. *Ultrasonics*, vol. 36, pp. 89–96.

Bahi, S.; Nouari, A.; Moufki, A.; El Mansori, M.; Molinari, A. (2011): A new friction law for sticking and sliding contacts in machining. *Tribology I.,* vol. 44(7-8), pp. 764–771.

Davis, C.D.; Hunter, S.C. (1960): Assessment of the strain rate sensitivity of metals by indentation with conical indenters. *J. Mech. Phys. Sol.*, vol. 8, pp. 235–254.

Demiral, M.; Roy A.; Silberschmidt, V. V. (2010): Effect of loading conditions on deformation process in indentation. *Comp., Mater.&Cont.*, vol. 19(2), pp. 199-216.

Garrido Maneiro, M. A.;Rodriquez, J. (2005): Pile-up effect on nanoindentation tests with spherical-conical tips. *Scripta Mater.*, vol. 52, pp. 593-598.

Gouldstone, A.; Chollacoop, N.; Dao, M.; Li, J.; Minor, A.M.; Shen, Y.-L.(2007): Indentation across size scales and disciplines: Recent developments in experimentation and modeling. *Acta Mater.*, vol. 55(12), pp. 4015–4039.

Kolsky, H. (1949): An investigation of the mechanical properties of materials at very high rates of loading, *Proc. R. Soc. London*, vol. 62, pp. 676–700.

Lu, J.; Suresh S.; Ravichandrana, G. (2003): Dynamic indentation for determining the strain rate sensitivity of metals. *J. Mech. Phys. Sol.*, vol. 51, pp. 1923-1938.

Mitrofanov, A. V.; Ahmed, N.; Babitsky, V. I.; Silberschmidt, V. V. (2005):

Effect of lubrication and cutting parameters on ultrasonically assisted turning of Inconel 718. *J. Mater. Process. Technol*, vol. 162-163, pp. 649-654.

Mok, C.H.; Duffy, J. (1965): The dynamic stress–strain relation of metals as determined from impact tests with a hard ball. *Int. J. Mech. Sci.,* vol. 7, pp. 355–371.

MSC, Marc User's Guide (2011). MSC Software Corporation, Version 2011, Los Angeles.

Ozel, T. (2006): The influence of friction models on finite element simulations of machining. *I. J. Mach. Tools and Manuf.*, vol. 46(5), pp. 518-530.

Suresh, S.; Giannakopoulos A. E. (1998): A new method for estimating residual stresses by instrumented sharp indentation. *Acta Mater.*, vol. 46, pp. 5755-5767.

Tirupataiah, Y.;Sundararajan, G. (1991): A dynamic indentation technique for the characterization of the high-strain rate plastic-flow behavior of ductile metals and alloys. *J. Mech. Phys. Solids*, vol. 39, pp. 243–271.

Zorev, N.N.; Shaw, M. C. (1996): *Metal Cutting Mechanics.* Pergamon Press, USA.